JOURNAL OF CATALYSIS **161,** 776–782 (1996)
ARTICLE NO. 0240

Methanol Synthesis and Reverse Water–Gas Shift Kinetics over Cu(110) Model Catalysts: Structural Sensitivity

Jun Yoshihara and Charles T. Campbell

Department of Chemistry, University of Washington, Box 351700, Seattle, Washington 98195-1700

Received December 13, 1995; revised February 29, 1996; accepted March 18, 1996

The kinetics of simultaneous methanol synthesis and reverse water–gas shift from CO_2/H_2 and $CO_2/CO/H_2$ mixtures have been measured at low conversions over a clean Cu(110) single-crystal surface at pressures of 5.1 bar. Without CO, $\sim 8 \times 10^{-3}$ methanol molecules per second per Cu surface atom were produced at 530 K, with an activation energy of 67 ± 17 kJ/mol; and $\sim$5 CO molecules per second per Cu surface atom were produced, with an activation energy of 78 ± 14 kJ/mol. The rates, compared to previous rates on Cu(100) and polycrystalline copper foil, were higher in both methanol synthesis and CO production, indicating structural sensitivity. The activation energy for methanol synthesis was similar on all these planes, but smaller for reverse water–gas shift on Cu(110) than on polycrystalline Cu. The surface after reaction was covered by almost a full monolayer of adsorbed formate, but no other species like carbon or oxygen in measurable amounts. The addition of CO to the feed caused the rate to increase, and no buildup of tenacious carbon was observed following reaction. Postreaction TPD shows an interesting influence of CO on the nature of the adlayer. These results support a model where the active site for methanol synthesis on real Cu/ZnO catalysts is metallic Cu and suggest that the role of ZnO may be to maintain more of the metallic Cu in ultrathin islands that have (110)-like behavior.

I. INTRODUCTION

Commercially, methanol is produced from synthesis gas ($CO/CO_2/H_2$) mainly over copper/zinc oxide catalysts (1–3). Both methanol synthesis, reaction [1], and water gas shift, reaction [2], take place simultaneously:

$$CO_2 + 3H_2 \rightarrow CH_3OH + H_2O, \quad [1]$$

$$H_2O + CO = CO_2 + H_2. \quad [2]$$

There has been extensive research on copper-based methanol synthesis catalysts, but the nature of the active center still remains subject to some controversy. It is well accepted that these catalysts contain metallic copper particles supported on a defected ZnO phase (4–32). However, it has often been proposed that the active site in methanol synthesis is a Cu^+ species dissolved in or supported on the ZnO phase (20, 22–40). Several groups have reported Cu-site-specific rates over SiO_2-supported Cu that are orders of magnitude below those generally reported for Cu/ZnO (22, 26–28, 54–56). These results are often interpreted as proving that the zinc component is essential in its catalytic activity and the role of the zinc-oxide support is to stabilize Cu^+ species.

On the other hand, some workers have been unable to identify significant amounts of Cu^+ (41–48) or even absorbed oxygen (3, 48) on the surface of working catalysts using techniques that should be sensitive to such species. Several groups show a reasonably good linear correlation between the metallic Cu surface area and the activity of a series of Cu/ZnO or $Cu/ZnO/Al_2O_3$ catalysts (5, 45, 46, 49–53), and others report a similar activity per Cu metallic surface area, irrespective of whether the Cu is supported on ZnO or SiO_2 (5, 50, 38, 57). Specific activities for Cu on a given support, particularly silica, vary widely from group to group (26, 27, 38, 56, 57), and depend on whether CO_2 is in the feed (2, 3, 57). There are well-known difficulties associated with measuring the Cu area of these catalysts (3, 11, 61–63) and maintaining that area clean and constant during reaction (3, 11, 41, 44, 53, 64). Because of these difficulties, we have made the rate measurements here on a Cu(110) single crystal whose surface area is determined geometrically, using a microreactor attached to an ultrahigh vacuum surface analysis chamber where the integrity of the surface can be verified before and after reaction.

Szanyi *et al.* (28) have previously measured methanol production from $CO/CO_2/H_2$ mixtures over a Cu(100) single-crystal surface. Their rates were some four orders of magnitude below those of high-area Cu/ZnO catalysts when compared on a per Cu surface atom basis. Taken at face value, this result proves that the active site is not metallic Cu. However, there are several factors that bring into question such an interpretation of those results. First, the surface was contaminated with much tenacious carbon during the reaction. (See (60) for quantitation of the carbon level.) This carbon would poison the catalyst, which would explain the low rate observed even if metallic Cu were the active phase. This carbon may be a natural consequence of the chemistry involved on pure Cu, or it might be due to

0021-9517/96 $18.00

impurities somehow accumulated on the model catalyst's surface. Second, the kinetics on Cu(100) were measured at only 1 bar pressure (28), whereas the rates on Cu/ZnO catalysts to which they compared their rates were measured at 15 bar. (The reaction is high order in total pressure at these low pressures (16, 58), with the rate varying as the total pressure to the 2.4 power in a later study on Cu(100) at pressures between 1 and 4 bar (58).)

Rasmussen *et al.* (58, 59) have also measured methanol synthesis rates over Cu(100), using only CO_2 and H_2 in the starting mixture, at a pressure of 1–4 bar. Their rates were only a factor of 10–100 below typical rates over real Cu/ZnO catalysts. They quantitatively attributed this to the difference in pressures used (58, 59) within a very reasonable microkinetic model for the reaction (59, 65). Furthermore, their sample showed no carbon impurity on the surface following reaction, but instead was covered by adsorbed formate, thought to be an intermediate in the reaction, and easily removed by heating in vacuum to the reaction temperature. Their results suggest that metallic Cu is the active species for methanol synthesis, completely opposite the conclusion from the earlier study on Cu(100) (28). The main difference is the addition of CO in the earlier study.

We recently reported (60) methanol synthesis kinetics over a clear polycrystalline Cu foil at pressures of 5 bar with a CO_2/H_2 mixture, which showed rates per Cu surface atom which are much higher than those measured in either study on Cu(100), but which are equal to those measured over real Cu/ZnO catalysts. We further reported the accompanying reverse water–gas shift kinetics and showed that the surface after reaction is covered by adsorbed formate, but no other species like tenacious carbon or oxygen in significant amount. These results support the results of Chorkendorff's group (58, 59) and suggest that the active site for methanol synthesis on real Cu/ZnO catalysts is metallic Cu.

One of the differences between these contradicting results is that one paper (28) had CO in its feed as well as CO_2 and H_2, while others (58–60) had only CO_2 and H_2. This leaves the possibility that metallic Cu can rapidly catalyze methanol production from CO_2/H_2 mixtures, but that the presence of CO poisons these metallic sites by the buildup of tenacious carbon. To clarify this point, we also study here the influence of added CO on the rate of methanol synthesis over Cu(110) and on the composition of this Cu surface after reaction.

In this paper, we report methanol synthesis and reverse water–gas shift (RWGS) reaction kinetics from $CO_2 + H_2$ over Cu(110). This open plane with its more coordinatively unsaturated Cu atoms is quite interesting in this respect because: (i) it is known to be considerably more active than Cu(111) in water–gas shift (66), and (ii) ultrathin islands of Cu on ZnO$(000\bar{1})$ show chemisorption properties much like Cu(110) (67–69), so that the catalytic activity of the Cu particles in real Cu/ZnO catalysts might also be expected to resemble this plane. We find here that methanol synthesis is structure sensitive, with this plane being more active than Cu(100) or polycrystalline Cu (mostly Cu(111)), and that this structure sensitivity is more dramatic in RWGS kinetics.

II. EXPERIMENTAL

The experiments were carried out in a batch microreactor attached to an ultrahigh vacuum (UHV) chamber for pre- and post-reaction surface analysis and sample cleaning. The sample was attached to a transfer rod for transport between these chambers and for resistively heating the sample. The microreactor was designed for higher pressures (up to 15 bar) and the sample repeatedly seals into this microreactor with a Teflon seat onto the rod that was diffusively separated from the sample. The sample and thermocouple were mounted on these electrical connections for resistive heating and temperature monitoring. It was proven that the clean sample could be moved from UHV chamber into the evacuated microreactor, sealed in it for long periods, and then returned to UHV without any significant buildup of surface species, as probed by X-ray photoelectron spectroscopy (XPS) and temperature-programmed desorption (TPD). The details of this system are given elsewhere (60, 70).

The sample was a 11.2-mm-diameter, 1-mm-thick copper (110) single crystal disk. A shallow groove was filed around the edge of the disk, and a 0.5-mm-diameter tungsten wire, formed in an horseshoe-shaped spring, was used to hold the disk. The tungsten wire was also used as a heating wire. Both ends of the tungsten wire were fixed to copper clamps attached to electrical feedthroughs at the end of the rod. The sample surface was initially polished to a mirror finish. The front of the sample was prepared prior to each reaction by argon sputtering and annealing to ~850 K, as specified previously for preparing a well-ordered Cu(110) surface (66, 71). Surface cleanliness was verified by highly sensitive XPS and TPD of test molecules. The sample retained its mirror finish throughout the course of these experiments.

The microreactor had a volume of about 58 ml, and it was used in the batch reactor mode (closed volume). The reaction was initiated by rapidly heating the sample to reaction temperature after introducing it into the microreactor and pressurizing the microreactor with the reaction mixture. A dry ice trap was used in the CO feedline to prevent metal carbonyls from entering the microreactor. The reaction was terminated by stopping the sample heating current, at which time it cooled rapidly toward room temperature and the reaction was quenched. The methods for rate determination by gas chromatography (GC) have been described previously (60).

Initially, the sample, sampleholder, and microreactor surface were passivated by heating the sample in ~1 mbar of a dilute H_2S in N_2 mixture in the microreactor. Afterward,

the sample's catalytic activity was also poisoned by the resulting monolayer of adsorbed sulfur, as seen previously (60, 71), but it was easily recovered by a very brief sputter cleaning that was sufficient to just barely remove most of the sulfur from the front surface. This control experiment proved that the catalytic rates we report here are due only to the front (110) surface of the Cu disk, but not due to its back or sides or the sample holder parts. After this series of kinetics experiments, a monolayer of sulfur was dosed to the front side of the sample in UHV using a directional doser with H_2S. This treatment passivated most of the sample's methanol and CO production activity, giving another proof that only the front side of the sample was active during kinetic measurements.

III. RESULTS

III.1. Pure $CO_2 + H_2$ Mixtures

Figure 1 shows an Arrhenius plot of methanol synthesis and reverse water–gas shift reaction rates over the clean Cu(110) surface, starting from a binary gas mixture of CO_2 and H_2 ($CO_2/H_2 = 1/11$), at a total pressure of 5.1 bar. Each absolute rate here represents an average rate taken from several gas chromatographic measurements of the reactor composition at several different reaction times up to 120 min. These represent conversions up to ~80 molecules of methanol and $\sim 10^5$ molecules of CO produced per surface Cu atom. The plot of these points versus time (not shown) was similar to that we presented previously, in that case for polycrystalline Cu (60). As can be seen, the RWGS reaction is roughly 3 orders of magnitude faster than methanol synthesis over Cu(110). Activation energies derived from this plot were 67 ± 17 kJ/mol for methanol synthesis and 78 ± 14 kJ/mol for the RWGS reaction. Figure 1 also includes our previous data over a polished polycrystalline copper foil, or Cu(poly), in the same reaction mixture, from (60). Methanol synthesis rates over high-surface-area Cu/ZnO catalysts in pure $CO_2 + H_2$ mixtures at 17–50 bar, taken from (2a, 38), are also plotted for comparison.

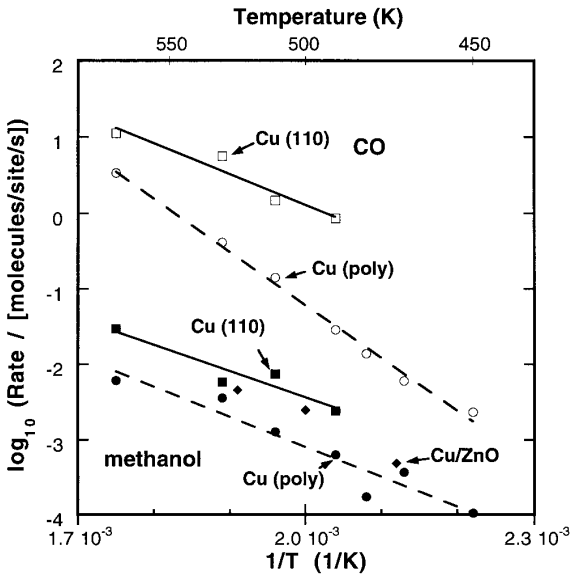

FIG. 1. Arrhenius plot of turnover frequencies for methanol synthesis and reverse water–gas shift over Cu(110) at 4.67 bar H_2 and 0.41 bar CO_2. Rates previously measured over a clean polyscrystalline Cu foil under these same conditions (60) and over high-area Cu/ZnO catalysts in pure $CO_2 + H_2$ feeds at total pressures from 17 to 50 bar are plotted for comparison, from (2a, 38). In calculating these absolute rates, it was assumed that the Cu(poly) sample had the same packing density as Cu(111), or 1.76×10^{15} Cu sites per cm^2, which is 63% greater than the Cu(110) packing density of 1.08×10^{15} Cu atoms per cm^2.

As can be seen, the RWGS reaction is much faster on the Cu(110) single-crystal surface compared to the polycrystalline surface, on which (111) facets should dominate (because they are the most stable thermodynamically, and that sample had been annealed at 850 and 900 K). This effect is even more significant at a lower temperature, with Cu(110) showing a smaller activation energy (78 ± 14 kJ/mol from the slope here) than polycrystalline copper (135 ± 5 kJ/mol (60)).

Similarly, methanol synthesis rates are obviously faster on Cu(110) than on Cu(poly) but the difference here is only a factor of ~3. An activation energy of 67 ± 17 kJ/mol was obtained here on Cu(110), close to that of 77 ± 10 kJ/mol over polycrystalline copper (60). This implies that these two reactions have different rate-limiting steps, with one quite sensitive and other rather less sensitive to the surface plane of the copper catalyst. In the RWGS reaction, the rate-determining step under these conditions is probably CO_2 dissociation (71), so it is not surprising that it shows structure sensitivity with the (110) plane being more active. Dissociative adsorption is generally more rapid on faces with a higher degree of coordinative unsaturation of the metal atoms.

As seen on Cu(100) (58, 59, 72) and in our previous study on Cu(poly) (60), a high coverage of adsorbed formate was found in postreaction analysis after methanol synthesis under $CO_2 + H_2$ mixtures. Figure 2 shows a TPD spectra from Cu(110) after reaction with the same mixture as in Fig. 1 at 530 K. The TPD peaks at ~475 K represent the decomposition of adsorbed formate, which releases CO_2 and H_2 nearly simultaneously in a 2 : 1 ratio at this temperature on pure Cu surfaces (68, 73–76). The small peaks below 350 K are thought to be due to outgassing from the sample heating wires. After the TPD spectrum was stopped at 600 K and the sample was recooled in UHV, no contamination on the surface was detected with XPS, and the spectrum was that of a clean Cu(110) surface.

For comparison with Fig. 2, the postreaction TPD spectrum from the Cu(poly) surface under these same conditions is reproduced in Fig. 3a. In addition, the TPD spectrum

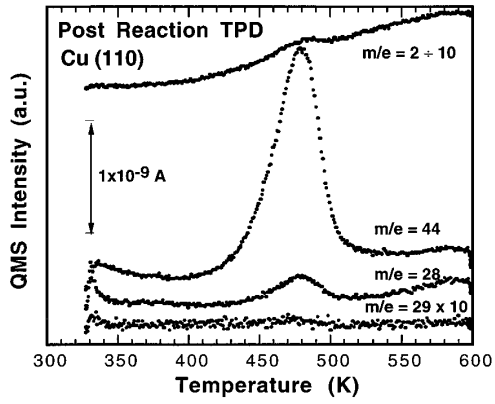

FIG. 2. Postreaction TPD from Cu(110). Reaction conditons: 530 K, 5.1 bar total pressure, 4.67 bar H_2, and 0.41 bar CO_2. Heating rate = 5 K/s.

after a saturation exposure (several Langmuirs) of formic acid to Cu(poly) at 300 K is shown in Fig. 3b. This exposure is known to produce adsorbed formate on Cu surfaces (68, 72–76), giving an absolute coverage of 3.4×10^{14} formates cm^2 in the case of Cu(110) (73). This TPD spectrum from formic acid shows typical formate decomposition peaks for pure Cu surfaces, desorbing H_2 and CO_2 nearly simultaneously at 475 K (68, 73–76). (While peak temperatures for

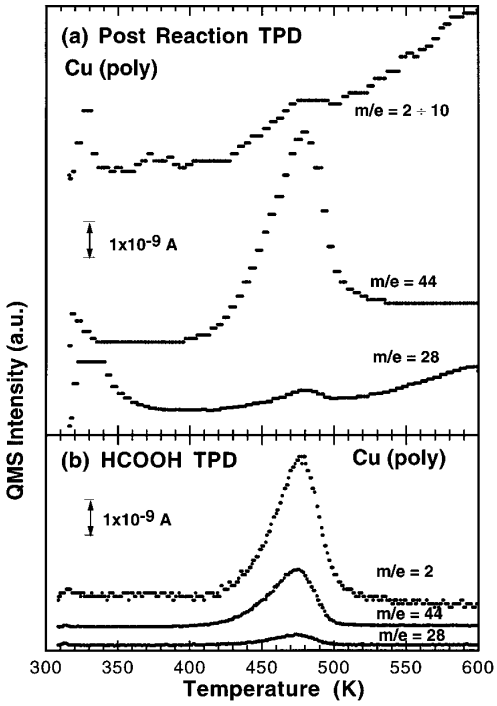

FIG. 3. (a) Postreaction TPD from Cu(poly) at 530 K, 5.1 bar total pressure, 0.41 bar CO_2, and 4.67 bar H_2. (b) TPD spectrum on same intensity scale following a saturation dose of formic acid to Cu(poly) at room temperature. This dose is known to produce adsorbed formate (HCOO) at high coverage.

formate decomposition near 475 K have been reported numerous times for Cu(110) (73–75) and Cu(100) (76), a peak temperature of only 430 K was once reported on Cu(100) (72).) The postreaction spectrum on Cu(poly) showed a slightly broader shoulder on the low-temperature side than the spectrum produced by adsorbing HCOOH. The H_2 background and outgassing from the sample transfer rod was also larger after the reaction, due to the exposure to such high H_2 pressure. After these TPD experiments, stopping at 600 K, no C or O were found on the Cu(poly) surface, as with Cu(110) above.

All these TPD spectra in Figs. 1 and 2 were collected with the same mass spectrometer multiplier voltage and with its ionization source located near the magic angle (to minimize intensity variations due to possible differences in angular distributions (77). Thus, the intensities should be directly comparable. However, the postreaction TPD intensities, which were collected over a period of some months, varied by a factor of ~2, probably due to changes in the multiplier sensitivity, the pumping speed of the system (which has a titanium sublimation pump), and wall pumping effects. We show here only spectra with the largest intensities. On average, the post-reaction TPD peaks from Cu(poly) were about twice as intense as those shown in Fig. 2b after formic acid saturation. The postreaction TPD peak areas were also larger from Cu(poly) than from Cu(110), by an average factor of ~2.5. While this is partially due to the 33% larger surface area for the Cu(poly) sample (1.3 vs 0.98 cm^2), the remaining significant difference suggests a greater number of surface sites per square centimeter on Cu(poly) than on Cu(110). This is consistent with the expectation that Cu(poly) is dominated by Cu(111) facets, which have a 63% higher packing density of Cu atoms than Cu(110).

The TPD intensity comparisons in Figs. 2 and 3 are intended mainly to show that adsorbed formate is present in near monolayer coverages after reaction on both Cu(110) and Cu(poly), and that no other species are present in moderate amounts.

III.2. Mixtures of $CO_2 + H_2$ with CO Addition

Figure 4 shows methanol synthesis rates over clean Cu(110) with various initial CO pressures in the reactant mixture. The total pressure was kept at 5.1 bar, and the CO_2 pressure was kept at 0.41 bar while changing the CO pressure. The H_2 pressure consequently decreased slightly, from ~4.6 to 3.8 bar, as the CO pressure increased to ~0.8 bar. The reaction time and temperature were kept at 60 min and 530 K, respectively. The methanol synthesis rate increased by ~70% with CO partial pressure, in spite of the expected decrease accompanying the corresponding decrease in H_2 pressure (16, 51, 58). This result proves that pure metallic copper can catalyze methanol synthesis from $CO/CO_2/H_2$ mixtures even better than with pure CO_2/H_2. The

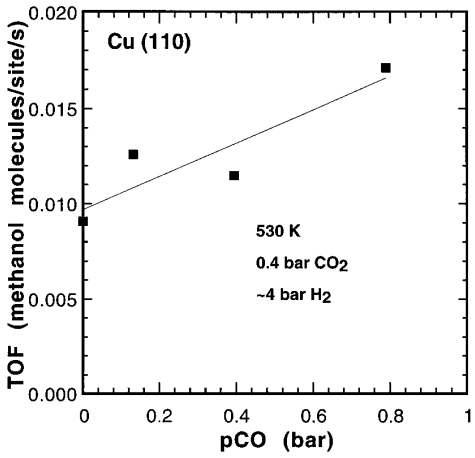

FIG. 4. Turnover frequency for methanol synthesis over Cu(110) as a function of initial CO partial pressure at 530 K, using a fixed total pressure 5.1 bar and a fixed CO_2 pressure of 0.41 bar, with the remainder H_2.

measurements in Fig. 4 were extended up to ~1.42 bar of CO, although the GC analysis above 0.8 bar was complicated by the increased intensity in the tail of the $CO + CO_2$ peaks. The steeper slope of this tail prevented the GC integrator from giving a methanol peak area of CO pressures above 0.8 bar, so data above 0.8 bar have not been included here. However, the methanol peak visually appeared to have an area within a factor of ~2 of those shown in Fig. 4 even at ~1.4 bar CO.

We detected no tenacious carbon buildup on the surface after the reaction. The TPD spectra after the reaction with no CO in the feed, and with 0.135 and 1.42 bar of CO, are shown in Fig. 5. Without CO in the feed, it showed a high coverage of formate, with its characteristic CO_2 peak at 474 K. Whenever CO was present initially, a new $m/e = 28$ desorption peak appeared at 380 K, as well as a smaller formate decomposition peak in postreaction TPD. So far, we have not tried to assign the $m/e = 28$ peak at 380 K, although its cracking pattern indicates that it is due to CO and not species like methanol, formaldehyde, or formic acid. It is clearly not simply due to molecularly adsorbed CO, which desorbs well below room temperature from pure Cu surfaces when present alone (see Refs. in (78)). It may be due to CO stabilized by the coadsorbed formate. The size of this CO peak increased and that of the formate peak decreased with increasing CO pressure. At 1.4 bar CO pressure, the formate TPD peak appeared at ~440 K instead of ~475 K. At 0.8 bar CO, formate decomposition showed peaks for $m/e = 44$ at both 400 and 475 K, in comparable intensity.

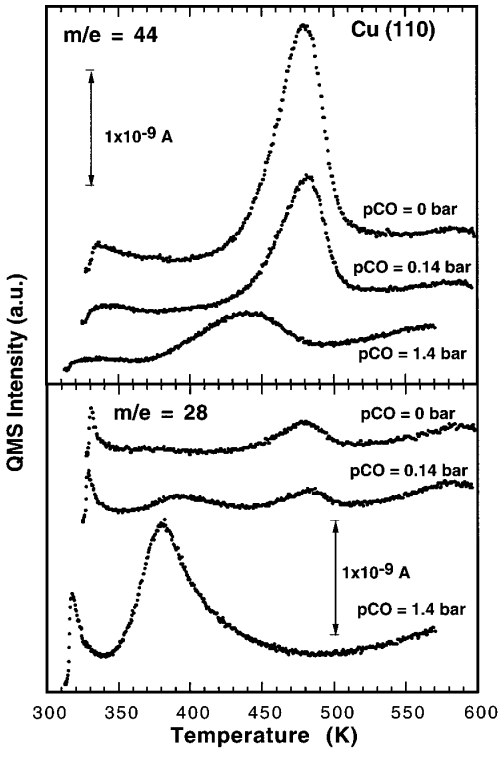

FIG. 5. Postreaction TPD from Cu(110): (a) without any CO, (b) with 0.135 bar CO replacing some of the H_2, and (c) with 1.42 bar CO replacing some H_2. Reaction conditions: ~530 K, 5.1 bar total pressure, 0.41 bar CO_2, remainder H_2.

IV. DISCUSSION

On Cu(110), the turnover frequency at 510 K in 5.1 bar total pressure of pure $CO_2 + H_2$ is $\sim 6 \times 10^{-3}$ site^{-1} s^{-1}, taken from the line in Fig. 1. This turnover frequency for Cu(110) at 510 K is in the range (4×10^{-3} to 1×10^{-2} site^{-1} s^{-1}) reported for the best high-area Cu/ZnO catalysts at this temperature and higher pressures (32–50 bar) with both CO and CO_2 in the feed (17, 19, 45, 51, 57). As shown above, the addition of CO gives even higher rates on Cu(110). The rates on Cu(110) are faster than those plotted in Fig. 1 for high-area Cu/ZnO catalysts measured in pure $CO_2 + H_2$, also at higher pressures. Higher pressures give higher rates, with a reaction order in total pressure of between 1.0 and 2.4 in this pressure range (16, 51, 58, 59). Thus, these comparisons prove that Cu(110) is at least as active as the best high-area Cu/ZnO catalysts, when compared on a per Cu surface atom basis.

The reaction rates reported here show that Cu(110) is more active than Cu(poly) in both methanol synthesis and the RWGS, with the effect being larger in the latter case. The Cu(poly) sample is probably dominated by Cu(111) facets, since these are most stable. Thus, methanol synthesis is mildly structure sensitive, whereas the RWGS is strongly structure sensitive. It was previously shown that the water–gas shift and RWGS reactions were structure sensitive, with higher activities and lower activation energies on Cu(110) than (111) by amounts similar to those observed here (66, 71). The absolute rate measured here for the

RWGS at 573 K, 0.41 bar CO_2, and 4.67 bar H_2 of ~11 site^{-1} s^{-1} can be compared to that we reported previously over Cu(110) at 573 K, 0.41 bar CO_2, and 1.0 bar H_2 of ~1.7 site^{-1} s^{-1} (71). When corrected for the lower H_2 pressure used previously assuming first-order behavior, these rates agree within 40%. The activation energies measured in that previous study (70 and 75 ± 8 kJ/mol (71)) also are very close to that measured here for the RWGS (78 ± 14 kJ/mol).

Rasmussen *et al.* (58) showed that the rate of methanol synthesis in 4 bar of a mixture of $1:1\ CO_2 + H_2$ over Cu(100) is $\sim 5 \times 10^{-4}$ per Cu surface atom per second at 543 K. This is considerably lower than the rate over Cu(110) of 1.3×10^{-2} per Cu surface atom per second taken from Fig. 1 at this same temperature and 5.1 bar total pressure. Again, this supports a structural sensitivity in methanol synthesis over Cu.

The higher rates for Cu(110) in methanol synthesis compared to Cu(100) and Cu(poly) suggest one possible beneficial role for ZnO in industrial catalysts, beyond simply maintaining the Cu in high dispersion. Since ultrathin films of Cu on ZnO have chemisorption properties closer to Cu(110) than Cu(111) or (100) (67–69, 78), the Cu in Cu/ZnO catalysts may be maintained in a metallic form that also more closely resembles this more active Cu(110) plane in its catalytic activity. Nakamura *et al.* (79) showed that addition of submonolayer Zn to a polished Cu foil surface caused the methanol synthesis rate at 523 K and 18 atm to increase by a factor of 3–6. One cannot rule out that this activity promotion also results from this same structural sensitivity, since the influence of the added Zn on the Cu surface morphology was not probed.

The apparent activation energies for methanol synthesis on Cu(100) (69 ± 4 kJ/mol (58)) and Cu(poly) (77 ± 10 kJ/mol, (60)) are very close to that measured here on Cu(110) of ~67 kJ/mol, in spite of the higher activity of the later.

Starting from a pure $CO_2 + H_2$ mixture, we show here that the replacement of up to 0.8 bar of the H_2 with CO causes the reaction rate to increase, in spite of the fact that the decrease in H_2 pressure should cause the rate to decrease up to ~40% (16, 51, 58, 59). This proves that under these conditions, the addition of CO has a weak positive influence on the net rate, and that it certainly does not cause carbon buildup which poisons the rate significantly. The absence of any tenacious carbon buildup following reaction in reaction mixtures with up to 1.42 bar CO further shows that CO does not dissociate to poison the surface with carbon.

The postreaction TPD spectrum changes upon addition of CO to the reaction mixture (see Fig. 5). It is unclear whether these changes are manifested in the reaction kinetics, since the coverages of these species may not be so high under reaction conditions, as suggested by a very reasonable kinetic model for the reaction (59, 65). The adsorbates which give rise to postreaction TPD peaks desorbing at *lower* temperatures than the reaction temperature are not necessarily populated to moderate coverages under the high-pressure reaction conditions, since they could be formed while cooling the sample. However, they easily could be populated at high coverages if the sticking portability to their creation is moderate, since the reactant pressures are high. Further study of the kinetics of formation of this interesting coadsorbed structure is needed.

As a point of reference, earlier studies on high-area Cu/ZnO catalysts have shown that the methanol synthesis rate decreased dramatically upon complete removal of CO_2 from the feed (i.e., in pure $CO + H_2$) (2, 3), consistent with tracer studies which showed that the *primary* source of carbon in the mechanism of methanol synthesis is CO_2, not CO (1, 3). We have not yet attempted rate measurements in pure $CO + H_2$, although based on these results one would expect that a much lower rate would be observed. Such an experiment on a clean Cu crystal would, however, be most interesting, since the rate might drop even more dramatically upon CO_2 removal than with high-area catalysts. This is because there is always some residual oxygen on the surfaces of high-area catalysts, which could easily convert to CO_2 (possibly mainly in some adsorbed carbonate or formate form on the catalyst's surface) under a $CO + H_2$ stream (or before). This residual CO_2 might be responsible for most of the residual rate observed in "pure" $CO + H_2$. This possibility could be more directly tested with a model catalyst of the type studied here.

ACKNOWLEDGMENTS

Financial support for this research by the Department of Energy, Office of Basic Energy Sciences, Division of Chemical Sciences, is gratefully acknowledged. J.Y. thanks the Mitsubishi Gas Chemical Company for a graduate fellowship and for partial financial support of this research. The authors thank Bruce Kay for suggestions on sample mounting.

REFERENCES

1. Chinchen, G. C., Denny, P. J., Parker, D. G., Spencer, M. S., and Whan, D. A., *Appl. Catal.* **30**, 333 (1987).
2. (a) Liu, G., Wilcox, D., Garland, M., and Kung, H. H., *J. Catal.* **90**, 139 (1984); Liu, G., Wilcox, D., Garland, M., and Kung, H. H., *J. Catal.* **96**, 251 (1985); (b) Lee, J. S., Lee, K. H., Lee, S. Y., and Kim, Y. G., *J. Catal.* **144**, 414 (1993).
3. Muhler, M., Törnqvist, E., Nielsen, L. P., Clausen, B. S., and Topsøe, H., *Catal. Lett.* **25**, 1 (1994).
4. Chinchen, G. C., Spencer, M. S., Waugh, K. C., and Whan, D. A., *J. Chem. Soc. Faraday Trans. I* **83**, 2193 (1987).
5. Chinchen, G. C., Denny, P. J., Jennings, J. R., Spencer, M. S., and Waugh, K. C., *Appl. Catal.* **36**, 1 (1988).
6. Kung, H. H., *Catal. Rev. Sci. Eng.* **22**(2), 235 (1980).
7. Ghiotti, G., and Boccuzzi, F., *Catal. Rev. Sci. Eng.* **29**(2&3), 151 (1987).
8. Roberts, D. L., and Griffin, G. L., *J. Catal.* **110**, 117 (1988).

9. Kau, L.-S., Hodgson, K. O., and Solomon, E. I., *J. Am. Chem. Soc.* **111**, 7103 (1989).
10. Clausen, B. S., Steffensen, G., Fabius, B., Villadsen, J., Feidenhans'l, R., and Topsøe, H., *J. Catal.* **132**, 524 (1991).
11. Muhler, M., Nielsen, L. P., Törnqvist, E., Clausen, B. S., and Topsøe, H., *Catal. Lett.* **14**, 241 (1992).
12. Fujita, S., Usui, M., Ohara, E., and Takezawa, N., *Catal. Lett.* **13**, 349 (1992).
13. Boccuzzi, F., Ghiotti, G., and Chiorino, A., *Surf. Sci.* **162**, 361 (1985).
14. Boccuzzi, F., Ghiotti, G., and Chiorino, A., *Surf. Sci.* **156**, 933 (1985).
15. Ghiotti, G., Boccuzzi, F., Chiorino, A., Che, M., and Bond, G. C., (Eds.), "Adsorption and Catalysis on Oxide Surfaces," p 235. Elsevier Amsterdam, 1985.
16. Agny, R. M., and Takoudis, C. G., *ACS Div. Fuel Chem.* **30**(2), 318 (1985).
17. Freidrich, J. B., Young, D. J., and Wainwright, M. S., *J. Catal.* **80**, 14 (1983).
18. Freidrich, J. B., Wainwright, M. S., and Young, D. J., *J. Catal.* **80**, 1 (1983).
19. Bridgewater, A. J., Wainwright, M. S., Young, D. J., and Orchard, J. P., *Appl. Catal.* **7**, 369 (1983).
20. Chanchlani, K. G., Hudgins, R. R., and Silveston, P. L., *J. Catal.* **136**, 59 (1992).
21. Millar, G. J., Rochester, C. H., Waugh, K. C., *J. Chem. Soc. Faraday Trans.* **88**, 1033 (1992).
22. Klier, K., *Adv. Catal.* **31**, 243 (1982).
23. Klier, K., *Appl. Surf. Sci.* **19**, 267 (1984).
24. Bulko, J. B., Herman, R. G., Klier, K., and Simmons, G. W., *J. Phys. Chem.* **83**, 3118 (1979); Herman, R. G., Klier, K., Simmons, G. W., Finn, B. P., Bulko, J. B., and Kobylinski, T. P., *J. Catal.* **56**, 407 (1979).
25. Mehta, S., Simmons, G. W., Klier, K., and Herman, R. G., *J. Catal.* **57**, 339 (1979); Dominguez, J. M., Simmons, G. W., and Klier, K., *J. Mol. Catal.* **20**, 369 (1983).
26. Nonneman, L. E. Y., and Ponec, V., *Catal. Lett.* **7**, 213 (1990).
27. Ponec, V., *Catal. Lett.* **11**, 249 (1991).
28. Szanyi, J., and Goodman, D. W., *Catal. Lett.* **10**, 383 (1991).
29. Okamoto, Y., Fukino, K., Imanaka, T., and Teranishi, S., *J. Phys. Chem.* **87**, 3747 (1983).
30. Gusi, S., Trifirò, F., Vaccari, A., and Del Piero, G., *J. Catal.* **94**, 120 (1985).
31. Visser-Luirink, G., Matulewicz, E. R. A., Hart, J., and Mol, J. C., *J. Phys. Chem.* **87**, 1470 (1983).
32. Sankar, G., Vasudevan, S., and Rao, C. N. R., *J. Chem. Phys.* **85**, 2291 (1986).
33. Apai, G. R., Monnier, J. R., and Hanrahan, M. J., *J. Chem. Soc. Chem. Commun.* **P84-003**, 212 (1984).
34. Apai, G., Monnier, J. R., and Preuss, D. R., *J. Catal.* **98**, 563 (1986).
35. Monnier, J. R., Hanrahan, M. J., and Apai, G., *J. Catal.* **92**, 119 (1985).
36. Apai., G., Monnier, J. R., and Hanrahan, M J., *Appl. Surf. Sci.* **19**, 307 (1984).
37. Bechara, R., Wrobel, G., Daage, M., and Bonnelle, J. P., *Appl. Catal.* **16**, 15 (1985).
38. Fujitani, T., Sato, M., Kanai, Y., Kakumoto, T., Watanabe, T., Nakamura, J., and Uchijima, T., *Catal. Lett.* **25**, 271 (1994).
39. Kanai, Y., Watanabe, T., Fujitani, T., Saito, M., Nakamura, J., and Uchijima, T., *Catal. Lett.* **27**, 67 (1994).
40. Yurieva, T. M., and Minyukova, T. P., *React. Kinet. Catal. Lett.* **29**, 55 (1985).
41. Goodby, B. E., and Pemberton, E., *Appl. Spectrosc.* **42**(5), 754 (1988).
42. Fleisch, T. H., and Mieville, R. L., *J. Catal.* **90**, 165 (1984).
43. Clausen, B. S., Lengeler, B., Rasmussen, B. S., Niemann, W., and Topsøe, H., *J. Phys.* **47**, C8-237 (1986).
44. Tohji, K., Udagawa, Y., Mizushima, T., and Ueno, A., *J. Phys. Chem.* **89**, 5671 (1985).
45. Pan, W. X., Cao, R., Roberts, D. L., and Griffin, G. L., *J. Catal.* **114**, 440 (1988).
46. Chiorino, A., Boccuzzi, F., and Ghiotti, G., *Surf. Sci.* **189/190**, 894 (1987).
47. Peplinski, B., and Unger, W. E. S., *Appl. Surf. Sci.* **62**, 115 (1992).
48. Moggridge, G. D., Rayment, T., Ormerod, R. M., Morris, M. A., and Lambert, R. M., *Nature* **358**, 658 (1992).
49. Shimomura, K., Ogawa, K., Oba, M., and Kotera, Y., *J. Catal.* **52**, 191 (1978).
50. Chinchen, G. C., Waugh, K. C., and Whan, D. A., *Appl. Catal.* **25**, 101 (1986).
51. Burch, R., Golunski, S. E., and Spencer, M. S., *Catal. Lett.* **5**, 55 (1990).
52. Denise, B., Sneeden, R. P. A., Beguin, B., and Cherifi, O., *Appl. Catal.* **30**, 353 (1987).
53. Robinson, W. R. A. M., and Mol, J. C., *Appl. Catal.* **60**, 73 (1990).
54. Burch, R., and Chappel, R. J., *Appl. Catal.* **45**(1), 131 (1988).
55. Leon y Leon, C. A., and Vannice, M. A., *Appl. Catal.* **69**, 305 (1991).
56. Burch, R., and Chappel, R. J., *Appl. Catal.* **45**, 131 (1988).
57. Robbins, J. L., Iglesia, E., Kelkar, C. P., and DeRites, B. A., *Catal. Lett.* **10**, 1 (1991).
58. Rasmussen, P. B., Kazuta, M., and Chorkendorff, I., *Surf. Sci.* **318**, 267 (1994).
59. Rasmussen, P. B., Holmblad, P. M., Askgaard, T., Ovesen, C. V., Stoltze, P., Norskov, J. K., and Chorkendorff, I., *Catal. Lett.* **26**, 373 (1994).
60. Yoshihara, J., Parker, S. C., Schafer, A., and Campbell, C. T., *Catal. Lett.* **31**, 313 (1995).
61. Denise, B., Sneeden, R. P. A., Beguin, B., and Cherifi, O., *Appl. Catal.* **30**, 353 (1987).
62. De Rossi, S., Ferraris, G., Mancini, R., *Appl.Catal.* **38**, 359 (1988).
63. Luys, M. J., Van Oeffelt, P. H., Pieters, P., and Ter Veen, R., *Catal. Today* **10**, 283 (1991).
64. van der Grift, C. J. G., Wielers, A. F. H., Joghi, B. P. J., van Beijnum, J., de Boer, M., Versluijs-Helder, M., and Geus, J. W., *J. Catal.* **131**, 178 (1991).
65. Askgaard, T. S., Norskov, J. K., Ovesen, C. V., and Stoltze, P., *J. Catal.* **156**, 229 (1995).
66. Nakamura, J., Campbell, J. M., and Campbell, C. T., *J. Chem. Soc. Faraday Trans.* **86**, 2725 (1990).
67. Campbell, C. T., and Ludviksson, A., *J. Am. Vac. Soc.* **A12**, 1825 (1994).
68. Ludviksson, A., Zhang, R., and Campbell, C. T., and Griffiths, K., *Surf. Sci.* **313**, 64 (1994).
69. Zhang, R., Ludviksson, A., and Campbell, C. T., *Catal. Lett.* **25**, 277 (1994).
70. Ludviksson, A., Yoshihara, J., and Campbell, C. T., *Rev. Sci. Instrum.* **66**(8), 4370 (1995).
71. Ernst, K.-H., Campbell, C. T., and Moretti, G., *J. Catal.* **134**, 66 (1992).
72. Taylor, P. A., Rasmussen, P. B., Ovesen, C. V., Stolze, P., and Chorkendorff, I., *Surf. Sci.* **261**, 191 (1992).
73. Henn, F. C., Rodriguez, J. A., and Campbell, C. T., *Surf. Sci.* **236**, 282 (1990).
74. Ying, D. H. S., and Madix, R. J., *J. Catal.* **61**, 48 (1980).
75. Bowker, M., and Madix, R. J., *Surf. Sci.* **102**, 542 (1981).
76. Dubois, L. H., Ellis, T. H., Zegarski, B. R., and Kevan, S. D., *Surf. Sci.* **172**, 385 (1986).
77. Pauls, S., and Campbell, C. T., *Surf. Sci.* **226**, 250 (1990).
78. Ludviksson, A., Ernst, K. H., Zhang, R., and Campbell, C. T., *J. Catal.* **141**, 380 (1993).
79. Nakamura, J., Nakamura, I., Uchijima, T., Kania, Y., Watanabe, T., Saito, M., and Fujitani, T., *Catal. Lett.* **31**, 325 (1995).